

**CHAPTER III**  
**SURFACE ENHANCED RAMAN SCATTERING OF N-(1-(2-  
CHLOROPHENYL)-2-(4-NITROPHENYL)ETHYL)-4-  
METHYLBENZENESULFONAMIDE (CNPSA) BY Ag NPs**

**Abstract**

SERS of N-(1-(2-chlorophenyl)-2-(4-nitrophenyl)ethyl)-4-methylbenzenesulfonamide (CNPSA) by Ag NPs was investigated using Raman spectroscopy. Ag NPs were synthesized by solution combustion method using citric acid as fuels. The prepared Ag NPs were characterized by XRD, UV, HR-TEM, FESEM and SERS studies. The prepared Ag NPs exhibit cubic crystalline structure with grain size 46nm. The surface plasmon resonance peak was found at 380nm. The spherical shape of Ag NPs was confirmed by FESEM and HR-TEM. The orientation of CNPSA molecule on Ag NPs has been inferred from nRs and SERS spectral feature. The molecule is adsorbed on the Ag NPs with the benzene ring in a tilted orientation. The presence of amino and sulfate group vibrations in the SERS spectrum reveal the interaction between amino and sulfate.

### **3.1 Introduction**

Sulfonamide based medicines were the second antimicrobial agents, still widely used today for the treatment of different bacterial, protozoal and fungal infections [1] and the first effective chemotherapeutic agents to be available in safe curative measure ranges [2]. They were the support of therapy for bacterial contaminations in human beings before the introduction of Penicillin in 1941 [3]. Compounds containing sulfonyl groups have long been a research focus as a result of their biological importance, chemical applications and some of the aryl sulfonamide derivatives are a common substructure class present in a large number of active pharmaceutical ingredients [4]. Sulfonamide derivatives occupy a unique position in the drug industry with their useful antibacterial and antimicrobial properties [5]. The applications of sulfonamides has greatly extended from their primary function as antitumor hypoglycemic anti-thyroid, anti-carbonic anhydrase, anti-inflammatory, diuretic, COX-inhibitors, dihydropteroate synthesise (DHPS)-the key enzyme involved in folate synthesis, anti-impotence drugs and also have been used as azo dyes for achieving improved light stability, water solubility, and fixation to fiber. Organic carbonates are valuable synthetic intermediate in medicinal, pharmaceutical industry and ubiquitously found in a variety of medicinal biologically active compounds [6-14]. In this present investigation, the effect of silver nanoparticles on the enhancement of SERS spectra and orientation of CNPSA molecule on the prepared Ag NPs were investigated.

### **3.2 Experimental**

#### ***3.2.1 Materials***

Silver nitrate ( $\text{AgNO}_3$ ), citric acid ( $\text{C}_6\text{H}_8\text{O}_7$ ) was purchased from MERCK. CNPSA molecule was synthesized according to the literature [15]. Double-distilled water was used throughout the experiment. All glassware's were properly washed with distilled water and dried in hot air oven before use.

#### ***3.2.2 Synthesis of Ag NPs using solution combustion method***

Ag NPs used in this study were synthesized by solution combustion method as discussed in chapter II.

### 3.2.3 Characterization

The Ag NPs were subjected to X-ray diffraction analysis (PAN alytical X'pert-PRO diffractometer system, Eindhoven, The Netherlands) and target was Cu  $K\alpha$  with a wavelength of 1.5406Å. The generator was operated at 40 kv and with a 30mA current. The scanning range was selected between 10° and 80°. The optical measurements were carried out using Shimadzu UV-1700 pharmaspec UV–visible spectrophotometer. The size, composition, and atomic structure of the NPs were analyzed by HR-TEM using a 200 kV JEOL JEM 2100 microscope with lattice resolution of 0.14nm and point-to-point resolution of 0.19nm. The samples were made by depositing the Ag NPs on a carbon coated Cu grid and the size measurements were performed manually on HR-TEM images. FESEM analysis was done using an advanced micro analysis solution AMETEK. The Raman spectra were recorded in the wavelength region 400–1100nm by micro-Raman system (Jobin Yvon Horiba LABRAM-HR visible) using He–Ne as excitation laser source at wavelength 632.8nm. Using confocal optics a lateral resolution of 1 micron and an axial resolution of 2 micron can be achieved. 600 and 1800 lines/mm gratings were used for dispersive geometry, the charge-coupled device (CCD) camera was used as the detector with the spectral resolution of  $1\text{cm}^{-1}$ . SERS spectra were recorded by mixing solid form of Ag NPs and CNPSA in 1:1 ratios. The experimental conditions are same for both normal Raman and SERS measurements.

## 3.3 Result and discussion

### 3.3.1 Structural studies of Ag NPs

The structure of prepared Ag NPs has been studied by XRD analysis. Figure 3.1 shows a typical XRD pattern of the prepared silver nanoparticles using citric acid as fuel in stoichiometric. The XRD peak positions were consistent the silver and the sharp peaks of XRD indicate the crystalline nature. The peaks were observed at  $2\theta = 38.1^\circ, 44.3^\circ, 64.4^\circ$  and  $77.4^\circ$  which correspond to (111), (200), (220) and (311) Bragg's reflections of face centre cubic (fcc) structure of silver respectively (JCPDS# 89-3722). The lattice constant values are also calculated and are very close to the standard data. The calculated lattice constants of the unit cells are  $a=4.084$ . No peak of other impurities has been detected from this pattern. This indicates that Ag was obtained under the present synthesis conditions. The particle size (D) of the Ag nanoparticles was calculated using the Debye–Scherrer formula as  $D=0.9\lambda / \beta \cos\theta$

where  $D$  is the particles size (nm),  $\lambda$  is the wavelength of the X-ray ( $\lambda = 1.5406 \text{ \AA}$ ),  $\beta$  is the full width at half-maximum intensity of the diffraction line (in radians) and  $\theta$  is the Bragg angle (degree) of the reflection peak. The calculated average particles size was found around 46nm.

### **3.3.2 Optical studies of Ag NPs**

The optical properties of prepared Ag NPs were characterized by UV–visible spectroscopy. Figure 3.2 shows the UV-visible absorption spectra of the Ag NPs in the range of 350-500nm. The appearance of surface plasmon peak at 380nm confirms the formation of Ag NPs. Ag NPs exhibit an intense absorption peak in the visible region due to the surface plasmon excitation. Surface plasmon resonance (SPR) absorption band is observed due to the combined oscillation of free conduction electrons of metal nanoparticles in resonance with light wave. This surface plasmon resonance peak depends on the particle size, shape, surface charge, separation between the particle and the nature of the environment [16]. The full-width at half maxima (FWHM) is reported to be quite useful in understanding the particle size and their distribution within the medium [17]. In the present work, the FWHM of the Ag NPs is observed at 10nm. The observed symmetric plasmon band shows that the silver NPs are spherical in shape which was also confirmed by TEM results.

### **3.3.3 Morphological Studies of Ag NPs**

The morphology and internal crystalline structure of obtained nanoparticles were studied by HR-TEM and SEM shown in figure 3.3 and 3.4. The TEM and SEM image illustrate that the Ag NPs were well dispersed with a little aggregation possessing almost spherical shape are observed in the image because of the escaping gases during combustion reaction. This may be due to escaping of gas with high pressure. The spherical shaped Ag NPs were found to be in range from 15-44nm these size of the particle confirms the nanoparticles. From the images which are evident that the morphology of Ag NPs is nearly spherical it is in agreement with XRD [18]. The EDS microanalysis is shown in figure.3.5 and confirms the presence of Ag NPs which is known to provide information on the chemical analysis of the elements or the composition at specific locations. The spectrum analysis reveals signal in the silver region and then confirms the formation of Ag NPs. Metallic silver nanocrystals generally show a typical optical absorption peak at approximately 3 keV due to the surface plasmon resonance [19-21]. This result confirmed the presence there of silver.

### 3.3.4 SERS studies

#### 3.3.4.1 Vibrational assignments

Figure 3.6 shows the structure of CNPSA molecule. Figure 3.7 shows the normal Raman spectrum (nRs) of CNPSA molecule. Figure 3.8 depicts the SERS spectrum of CNPSA molecule in silver nanoparticles. Table 3.1 shows the vibrational modes and corresponding assignments.

Generally, the C-C stretching (ring stretching) vibration mode occurs in the region  $1650\text{-}1300\text{cm}^{-1}$  [22, 23]. In the present case, the C-C stretching modes are observed in the region  $1629\text{-}1290\text{cm}^{-1}$  in both nRs and SERS. In benzene-like molecules C-H in-plane bending vibrations are observed in the region  $1300\text{-}1000\text{cm}^{-1}$  and are usually weak. The C-H out-of-plane bending mode of usually medium intensity arises in the region  $900\text{-}600\text{cm}^{-1}$  [23]. In the present case, C-H in-plane bending is observed in the region  $1290\text{-}990\text{cm}^{-1}$  in both nRs and SERS. The out-of-plane bending observed at  $962\text{-}608\text{cm}^{-1}$  in both nRs and SERS are assigned to C-H out-of-plane bending.

The identification of C-N and C=N vibration is a very difficult task, since the mixing of several bands are possible in this region [24] C-N stretching absorption is assigned in the region  $1382\text{-}1266\text{cm}^{-1}$  for aromatic amines. In our title molecule, three C-N stretching vibrations were possible and the bands are observed in the range  $1344\text{-}1207\text{cm}^{-1}$  in nRs and  $1350\text{-}1290\text{cm}^{-1}$  in SERS spectrum. N-H band in most important amides undergoes N-H deformation in the region  $1565\text{-}1475\text{cm}^{-1}$  [25]. In the present case, medium and weak vibrational mode occurring at  $1602\text{cm}^{-1}$  in nRs and at  $1602\text{-}1529\text{cm}^{-1}$  in SERS are assigned to N-H deformation mode.

commonly,  $\text{SO}_2$  in sulfonamide shows strong band for  $\text{SO}_2$  asymmetric and symmetric stretching vibration observed in the region  $1446\text{-}1433\text{cm}^{-1}$  and  $1214\text{-}1172\text{cm}^{-1}$  [26,27]. In this case, vibrational modes occurring at  $1417\text{cm}^{-1}$  in SERS are also assigned to  $\text{SO}_2$  asymmetric stretching and symmetric stretching  $\text{SO}_2$  vibrational modes that occur in the region  $1207\text{-}1187\text{cm}^{-1}$  in both nRs and SERS.  $\text{SO}_2$  deformation vibrational modes are observed in the region  $532$  and  $444\text{cm}^{-1}$  [28]. In the present case,  $\text{SO}_2$  deformation vibrational mode is observed  $541$  and  $466\text{cm}^{-1}$  in SERS. Sulfoxide SO stretching vibration appears in  $1350\text{cm}^{-1}$  depending upon the presence of substituent [28]. In the present case, peaks at  $1344\text{cm}^{-1}$  in nRs and at  $1350\text{cm}^{-1}$  in SERS are assigned to SO stretching.

Aromatic nitro compound have strong absorption due to the asymmetric and symmetric stretching vibration of the  $\text{NO}_2$  group at  $1570\text{-}1485\text{cm}^{-1}$  and  $1370\text{-}1320\text{ cm}^{-1}$  respectively. Hydrogen bonding has little effect on the  $\text{NO}_2$  asymmetric stretching [29, 30]. In the present case, the nRs band is observed at  $1602\text{cm}^{-1}$  and SERS bands occurring in the region  $1602\text{-}1529\text{cm}^{-1}$  are assigned asymmetric  $\text{NO}_2$  stretching vibrational mode and symmetric stretching of  $\text{NO}_2$  vibrational mode occurred in the region  $1344\text{cm}^{-1}$  in nRs and at  $1350\text{cm}^{-1}$  in SERS.

The C-Cl stretching vibration gives generally strong bands in the region  $730\text{-}580\text{cm}^{-1}$  in dihalogen substituted benzene derivatives [31]. In the present studies, the nRs bands are observed at  $634\text{cm}^{-1}$  and SERS bands occurs in the region  $714\text{-}608\text{cm}^{-1}$  are assigned to C-Cl stretching vibrational modes. The C-Cl in-plane bending vibrational modes are observed nRs band at  $304\text{cm}^{-1}$  and SERS is observed at  $302\text{cm}^{-1}$ . This is in agreement with the literature data [32-34].

Usually, the scissoring of  $\text{CH}_2$  band in the spectra of hydrocarbons occurs nearly at  $1465\text{cm}^{-1}$  while methylene twisting and wagging vibrations are observed in the region  $1350\text{-}1150\text{cm}^{-1}$  [35]. The SERS band in the region  $1417\text{cm}^{-1}$  is assigned to  $\text{CH}_2$  scissoring vibrations. The  $\text{CH}_2$  wagging vibrational mode occurs in the region  $1350\text{-}1152\text{cm}^{-1}$  in both nRs and SERS. The skeletal deformation vibrational mode occurs in the region  $600\text{-}250\text{cm}^{-1}$  [35]. The observed nRs band around  $427\text{-}270\text{cm}^{-1}$  and SERS band around  $541\text{-}278\text{cm}^{-1}$  are assigned to skeletal deformation of title molecule (CNPSA).

The band at  $226\text{cm}^{-1}$  is due to the stretching mode between metal and adsorbate. In most of the studies on oxygen heterocycles adsorbed on silver electrodes, this line is recognized as the weak Ag-O bond [36, 37]. In the present case, the SERS band observed at  $227\text{cm}^{-1}$  was assigned as Ag-O stretching vibrational mode.

#### **3.3.4.2 Orientation of CNPSA molecule and CNPSA molecule on Ag NPs**

The surface-enhancement depends on the following factors. The first effect is the kind of adsorption between chemical compounds and metal NPs, that is, chemisorptions or physisorption. Molecules chemisorbed on the metal surface show a larger enhancement than the physisorbed molecules, signifying some chemical effect between the molecule and the surface. It is known that the absorption coefficients of chemisorbed molecules are larger than those of condensed over layers [38]. The

second effect depends on the orientation of the chemical compound on the metal NPs, that is, flat-on or stand-on orientation. The third effect involves the polar replacement of the chemical compound, which indicates the electron retreating or donating groups [39, 40].

The orientation mechanism of a CNPSA can be deduced from its SERS spectrum through a detailed analysis of the peak shift and band broadening caused by the surface adsorption [41]. There are three potential orientations that the molecule may adsorb on metal nanoparticles such as face-on, tilted, and stand-on orientations. The orientation of the molecule on the Ag NPs can be inferred from aromatic C-H stretching vibrations, in-plane and out-of-plane vibrations, ring stretching, ring breathing and the SERS surface selection rule.

The surface selection rule suggests that for a molecule adsorbed flat on the Ag NPs, its out-of-plane vibrational modes will be more enhanced when compared with its in-plane vibrational modes and vice versa when it is adsorbed perpendicular to the surface [42, 43]. It is further seen that vibrations involving atoms that are close to the Ag NPs will be enhanced. When wavenumber difference between Raman bands in normal and SERS spectra is not more than  $5\text{cm}^{-1}$ , the molecular plane is expected to be perpendicular to the Ag NPs [44].

The SERS spectrum of title molecule, the C-N stretching mode is strongly enhanced, which indicates that the NH group interact more with metal nanoparticles [40]. This interaction causes weakening of the C-N bond. Hence more molecules are focused for absorption and are responsible for strong enhancement of C-N stretching in the spectrum. Usually, the C-N stretching vibrational modes are observed in the region  $1266\text{-}1382\text{cm}^{-1}$  [25]. In the present case, the C-N stretching vibrational modes are present in the region  $1350\text{-}1232\text{cm}^{-1}$  as a very strong band in the SERS spectrum. The presence of these C-N stretching modes indicates the interaction between the title molecule and the metal nanoparticles through the amino group. In this case, the deformation modes of the NH group at  $1602$  and  $1529\text{cm}^{-1}$  support the argument. Also the substituent sensitive vibrations at  $466\text{cm}^{-1}$  in the SERS spectrum support the interaction of amino group with the metal nanoparticles. The phenyl ring moiety of the CNPSA molecule is planar and is very well suited to  $\pi$ -bonding in a flat orientation. Since, the NH moiety is not planar, the phenyl ring moiety is not in a favoured position to make  $\pi$ -bonding in a flat orientation. Therefore the phenyl ring makes  $\pi$ -bonding with Ag NPs in a slightly increasing disposed position (tilted

orientation). Also the sulfate moiety with negative charge can make interactions with the Ag NPs. We have argued that those vibrations, which result in the most charge transfer in and out of the metal in synchronism with the nuclear motion accompanying them, will be most enhanced [45]. When  $\pi$ -bonded through the benzene ring, the ring vibrations become good candidates for such charge transfer, and should therefore be strongly present in the SERS spectrum.

The in-plane bending vibrations of the phenyl ring are observed at  $1290\text{-}990\text{cm}^{-1}$  and the out-of-plane bending modes are observed at  $962\text{-}608\text{cm}^{-1}$  in the SERS spectrum of the CNPSA compound suggest that there is a certain angle between the ring and the surface of the Ag NPs. The substitute in-plane and out-of-plane bending modes are also detected at the same time, suggesting a tilted orientation of the molecule [46, 47]. This leads to evidence for a tilted CNPSA molecule on Ag NPs.

The asymmetric and symmetric  $\text{SO}_2$  stretching vibrational modes are observed in region  $1417\text{-}1187\text{cm}^{-1}$  in the both nRs and SERS. This indicates that the  $\text{SO}_2$  group probably near to the metal nanoparticles. Similarly, the enhanced high intensity SERS band at  $1350\text{cm}^{-1}$  assigned for SO stretching vibrational mode. This again supports the possibility of direct interaction between the sulfate group and the Ag NPs. This is justifiable because the modes of groups directly interacting with the metal nanoparticles will be prominent in SERS spectrum and undergo a wavenumber shift [48, 49].

It has also been recognized in the literature [50] that when a benzene ring moiety interacts straight with a metal nanoparticles, the ring breathing mode is red shifted by  $10\text{cm}^{-1}$  along with substantial band broadening in the SERS spectrum. In the present case, the ring breathing mode is present at  $1111\text{cm}^{-1}$  without any wavenumber shift. Neither a considerable red shift nor important band broadening was identified in the SERS spectrum of the CNPSA compound meaning that the probability of an express ring  $\pi$ -orbital to metal interaction should be low, in accordance to a tilted position of the ring.

In SERS spectrum of title molecule in Ag NPs, the  $1629\text{-}1290\text{cm}^{-1}$  band, assigned to the C-C stretching of benzene are very strong, indicating that the interaction between benzene rings of title molecule and the surface of Ag NPs is strong. In the present case, the strong intense peak of SERS observed at  $1350\text{cm}^{-1}$  is upshifted by  $6\text{cm}^{-1}$  in nRs of CNPSA molecule for C-C stretching. The C-C stretching

mode observed in  $1602\text{cm}^{-1}$  spectrum, there is no shift of these band compared with the corresponding band in the nRs and SERS spectrum, indicating that it is still a physical interaction. This is an evidence for titled orientation of CNPSA molecule on the Ag NPs.

Apart from the interaction of the nitro group in the adsorption process, the SO group can also bind to the Ag NPs through the oxygen atom. In the case,  $\text{NO}_2$  symmetric stretching and SO stretching occurs in  $1344\text{cm}^{-1}$  in nRs of CNPSA and at  $1350\text{cm}^{-1}$  of the compound in SERS. The SERS peak at  $1350\text{cm}^{-1}$  is slightly increased in intensity and downshifted by  $6\text{cm}^{-1}$  than in nRs. It is an confirmation for orientation of the title molecule throughout the electron retreating  $\text{NO}_2$  group of the benzene ring in the organic molecule and through the lone pair of electron on SO. The motivation may be due to the polarizability tensor of these modes being normal to the surface and according to charge transfer and electromagnetic mechanism; the vibrational mode gets enhanced in intensity.

In this present case, a new band appears at  $227\text{cm}^{-1}$  in SERS which was due to Ag-O stretching vibration [38]. This indicates that the sulfied group was adsorbed on Ag NPs through the oxygen atoms in tilted orientation. The enhancement methyl scissoring ( $1417\text{cm}^{-1}$ ), wagging ( $1290\text{-}1152\text{cm}^{-1}$ ), skeletal deformation ( $541\text{-}348\text{cm}^{-1}$ ), chloride stretching ( $714\text{-}541\text{cm}^{-1}$ ) and C-Cl in-plane mode ( $302\text{cm}^{-1}$ ) and rocking mode ( $158\text{cm}^{-1}$ ) further support that the orientation of CNPSA molecule on Ag NPs is tilted orientation of the benzene ring moiety on the silver substrate. The observed high SERS signal indicates that the prepared silver nanoparticles are good source for biomedical applications as SERS substrate.

### **3.4 Conclusion**

Ag NPs were synthesized by solution combustion method using citric acid as fuels. The prepared Ag NPs were characterized by XRD, UV, TEM and SEM techniques to identify the size, shape of Ag NPs. Morphological studies show that the average size of the prepared Ag NPs was 15-44nm. Spherical shape of the prepared Ag NPs was as expected from XRD, UV, TEM and SEM measurements. The nRs and SERS spectra of CNPSA were studied. The presence of in-plane and out-of-plane modes of phenyl ring in the SERS spectrum suggest a tilted orientation of the molecule with respect to the Ag NPs. The presence of amino and sulfate group vibrations in the SERS spectrum show the interaction between these group and the Ag NPs.

## Reference

- [1] Z. Franca, V. Paola, *Archiv der Pharmazie.*, 331 (1998) 219.
- [2] S. Alyar, N. J. Karacan, *Enzyme Inhib. Med. Chem.*, 24 (2009) 986.
- [3] A. Camargo Ordonez, C. Moreno-Reyes, F. Olazaran Santibanez, S. Martinez Hernandez, V. Bocanegra Garcia, G. Rivera, *Quim. Nova.*, 34 (2011) 787.
- [4] D. A. Smith, R. M. Jones, *Curr. Opin. Drug Discov. Devel.*, 9 (2008) 72.
- [5] C. Hansch, P.G. Sammes, J. B. Taylor, *Comprehensive Medicinal Chemistry*; Pergamon Press: Oxford, (1990) 2 Chapter 7.1.
- [6] T. Owa, T. Nagasu, *Exp. Opin. Ther. Pat.*, 10 (2000) 1725.
- [7] C. W. Thornber, *Chem. Soc. Rev.*, 8 (1979) 563.
- [8] R. C. Ogden, C. W. Flexner, *Protease inhibitors in AIDS therapy*. New York, U.S.A: Marcel Dekker, (2001).
- [9] I. Nishimori, D. Vullo, A. Innocenti, A. Scozzafava, A. Mastrolorenz, C.T. Supuran, *Bio.org. Med. Chem. Lett.*, 15 (2005) 3828.
- [10] J. J. Li, D. Anderson, E. G. Burton, J. N. Cogburn, J. T. Collins, D. J. Garland, S. A. Gregory, *J. Med. Chem.*, 38 (1995) 4570.
- [11] A. E. Boyd, *Diabetes.*, 37 (1988) 847.
- [12] T. S. Claudiu, C. Angela, S. Andrea, *Med. Res. Rev.*, 23 (2003) 535.
- [13] P. Adams, F. A. Baron, *Chem Rev.*, 65 (1965) 567.
- [14] I. Vauthey, F. Valot, C. Gozzi, F. Fache, M. Lemaire, *Tetrahedron Lett.*, 41 (2000) 6347.
- [15] O. Khoumeri, M. Montana and T. Terme, P. Vanelle, P. First, *Tetrahedron.*, 64 (2008) 11237.
- [16] U. Kreibig, M. Vollmer, *Optical Properties of Metal Clusters*, Springer, Verlag, Berlin, (1995).
- [17] K.R. Brown, D.G. Walter, M.J. Natan, *Chem. Mater.*, 12 (2000) 306.
- [18] J.L. Garda, E. Torresdey, J.R. Gomez, J.G. Peralta videa, H. Parsons, M. Troiani, J. Yacaman, A. Alfalfa sprouts, *Langmuir.*, 19 (2003) 1357.
- [19] S.L. Lui, V.K.M. Poon, I. Lung, A. Burd, *J. Medi. Micro.*, 55 (2006) 59.
- [20] H. Bar, D.H. Bhui, P.G. Sahoo, P. Sarkar, P.S. De Misra, *Coll. Surf. A Physicochem. Eng. Asp.*, 339 (2009) 134.
- [21] P. Magudapathy, P. Gangopadhyay, B.K. Panigrahi, K.G.M. Nair, S Dhara, *Physica B.*, 299 (2001) 142.
- [22] A. Sabur, M. Havel, Y. Gogotsi, *J. Raman Spectrosc.*, 39 (2008) 61.

- [23] A. Fathia Alseroury, J. Basic Appl. Sci., 5 (2011) 611.
- [24] G. Raja, K. Saravanan, K. Sivakumar, Int. J. Appl. Phys. Maths., 1 (2011) 2.
- [25] S. Cilverstein, M. Basseler. C. Morill C, Spectromertic identification of organic compounds., (wiley, NewYork) (1981).
- [26] B. Joseph, Introduction to Organic Spectroscopy, Macmillan Publications., New York, (1987).
- [27] A. Givan, A. Loewenschuss, C.J. Nielsen, J.Mole. struct., 604 (2002) 147.
- [28] P.L.Anto, R. J. Anto, H.T. Varghese, C.Y.Panicke, D.Philip., A.G. Brolo, J of Raman Spectrosc., 40 (2009) 1810.
- [29] N. Edayadulla, P. Ramesh, Med. Chem. Res., 21 (2012) 2056.
- [30] M. Arivazhagan, S. Jeyavijayan, Indi. J Pure & Appl Phys., 49 (2011) 516.
- [31] D. N. Sathyanarayana, Vibratiional Spectroscopy Theory and Application, New Age Inte rnational Publishers, New Delhi, (2004).
- [32] G Varasanyi, assignments for Vibratiional spectra od Seven Hundred Benzene derivatives, (1974) 1.
- [33] O. William George, S. Peter, McIntyre, D. J. Mowthorpe, infrared Spectrosc., John Wiley, I ed, (1987).
- [34] P.B. Nagabalasubramanian, M. Karabacak, S. Periandy, Spectrochimi., Acta part A. 85 (2012) 43.
- [35] A. Palafox, M. Rastogi, V. K. Mittal, Int J Quantum Chem. 94 (2003) 189.
- [36] M. Umadevi, P. Vanelle, T. Terme and V. Ramakrishnan, J. Raman. Spectrosc., 34 (2003) 172.
- [37] A.K. Ojha, A. Singh, S.Dasgupta, R.K. Singh, A. Roy, Chem. Phys. Letter., 431 (2006) 121.
- [38] P.S. Mdluli, N.M. Sosibo, N. Revrapasadu, P. Karmanis, J. Leszczynski, J. Mol. Struct., 935 (2009) 32.
- [39] P. Dumas, R. G. Tobin, P. Richards, Surf. Sci., 171 (1986) 555.
- [40] K. Geetha, M. Umadevi, G.V. Sathe, P. Vanelle, T. Terme, O. Khoumeri, J. Mole. Stru., 1059 (2014) 87.
- [41] N. Goutev and M. Futamata, Appl. Spectros., 57 (2003) 506.
- [42] A. G. Mal shukov, Phys. Rep., 194 (1990) 343.
- [43] J.A. Creighton, Spectroscopy of Surfaces Advances in Spectroscopy, John Wiley and Sons Inc., New York, (1988).
- [44] X. Gao, J.P. Davies, M.J.Weaver, J. Phys. Chem. A., 94 (1990) 6858.

- [45] G. Levi, J. Patigny, J.P. Massault, J. Aubard, Thirteenth International Conference on Raman Spectroscopy., Wurzburg, (1992) 652.
- [46] D. P. DiLella, M. Moskovits, J. Phys. Chem., 85 (1981) 2042.
- [47] D. Philip, A. John, C.Y. Panicker, H.T. Varghese, Spectrochim. Acta., 57 (2001) 1561.
- [48] K. Eckhard, J.K. Bert, J.M. Robert, J. Phys. Chem. 100 (1996) 5078.
- [49] S. Kai, W. Chaozhi, X. Guangzhi, Spectrochim. Acta., 45 (1989) 1029.
- [50] S. Trasatti, J. Electroanal. Chem., 33 (1971) 351.

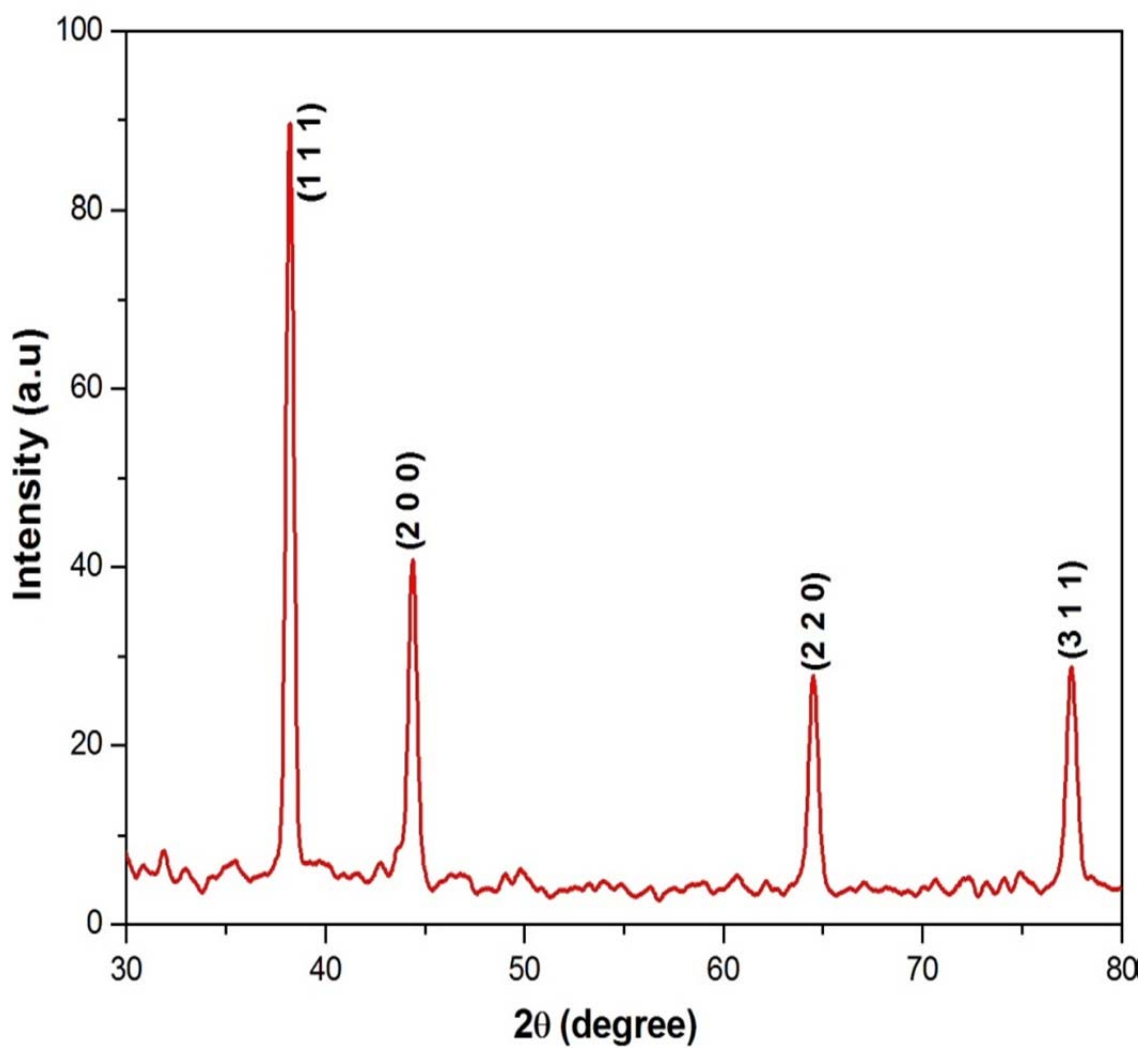


**Figure 3.1** X-Ray diffraction pattern of prepared Ag NPs.

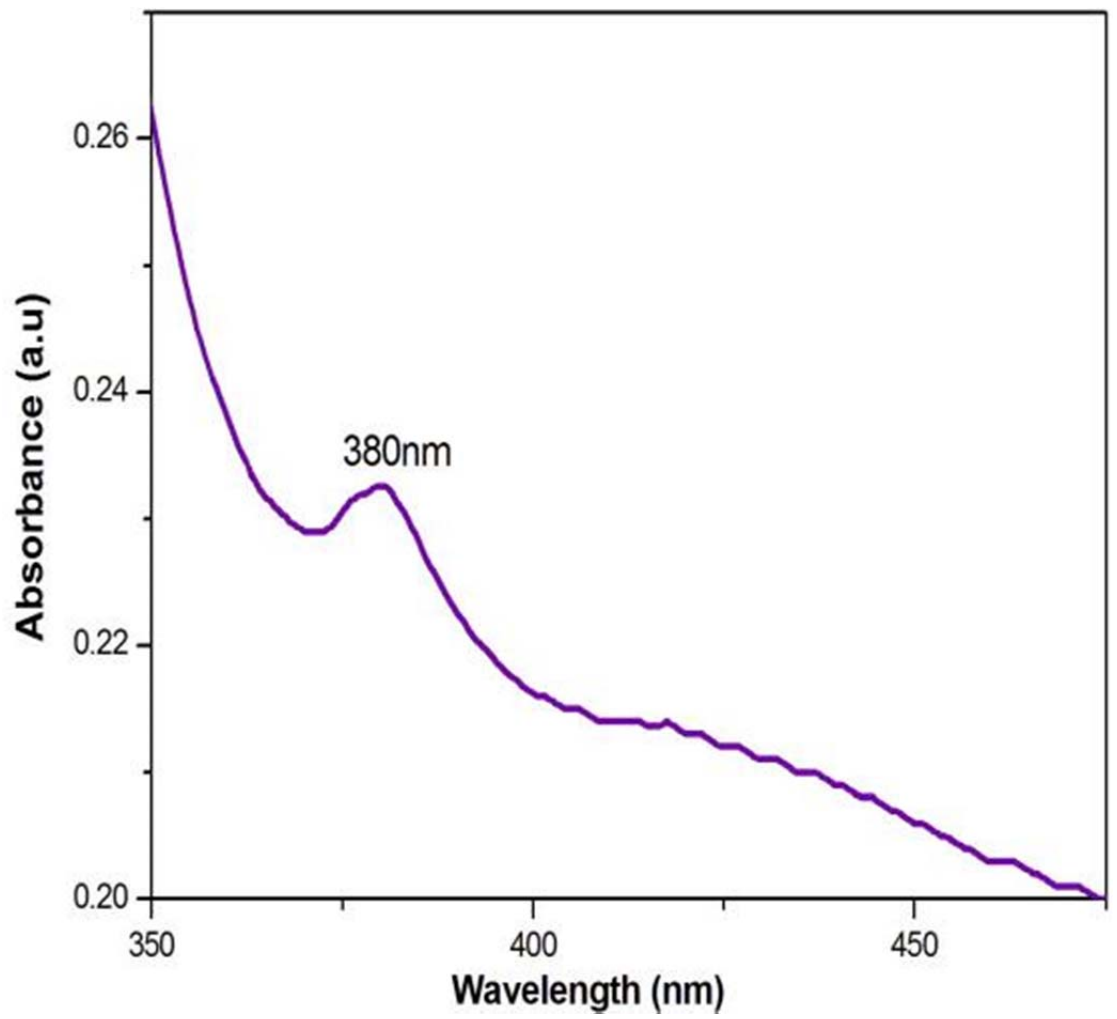


**Figure 3.2** UV-Visible spectrums of prepared Ag NPs.

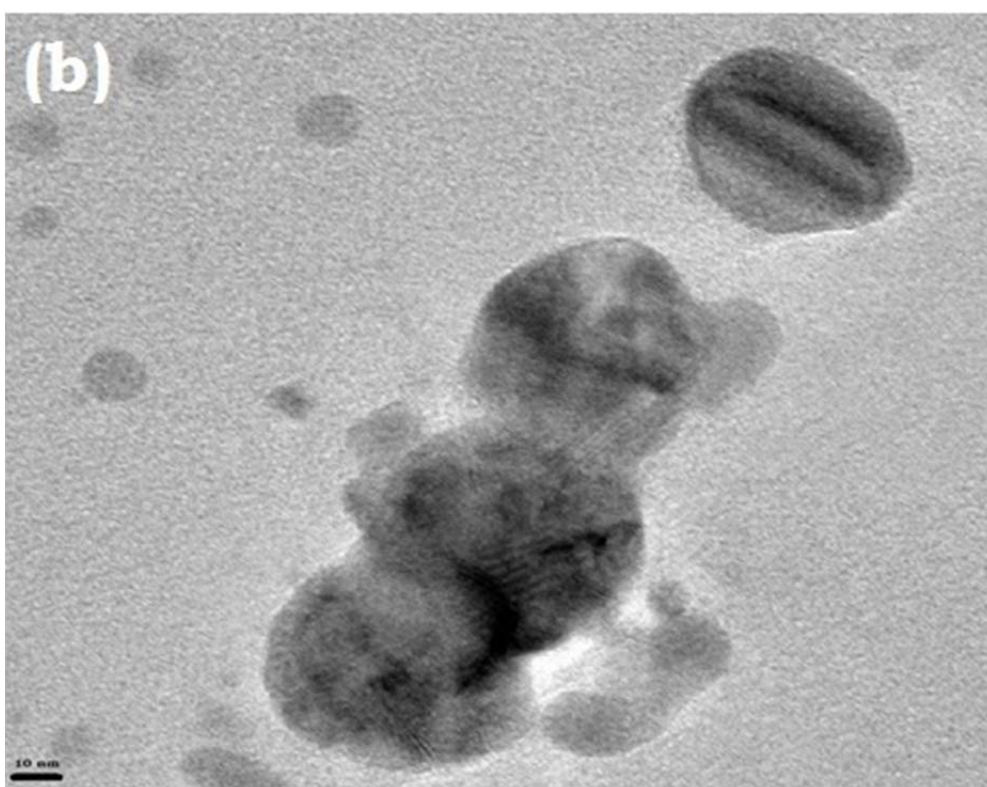
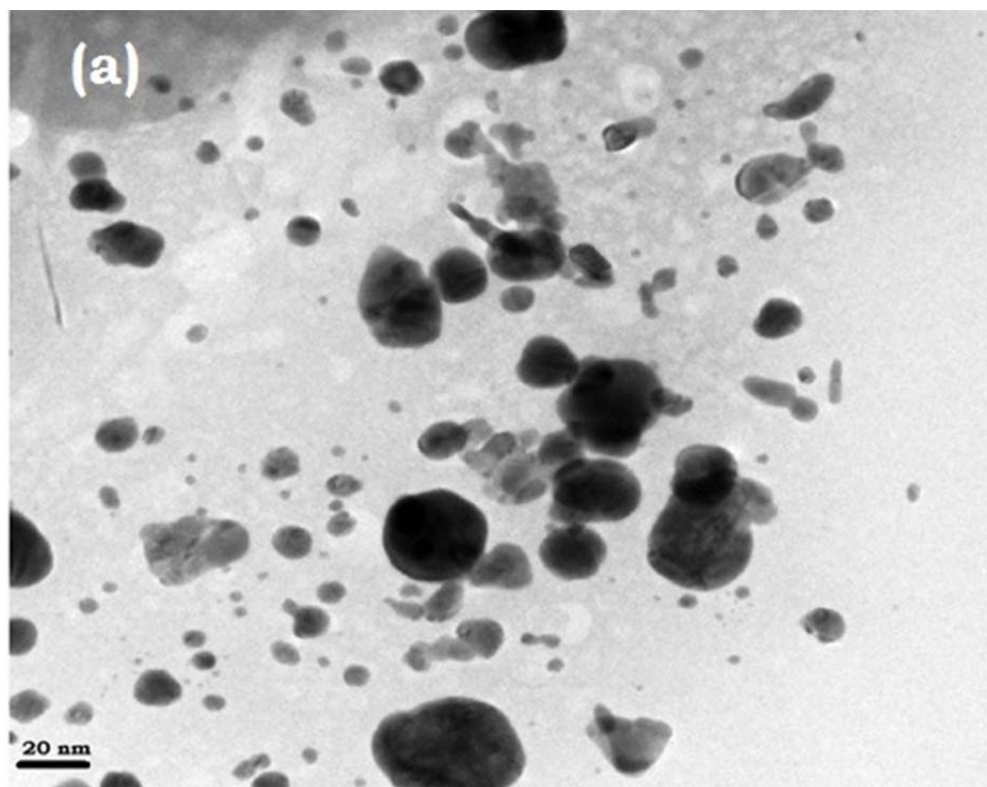


**Figure 3.3** HR-TEM images of prepared Ag NPs in different magnifications.

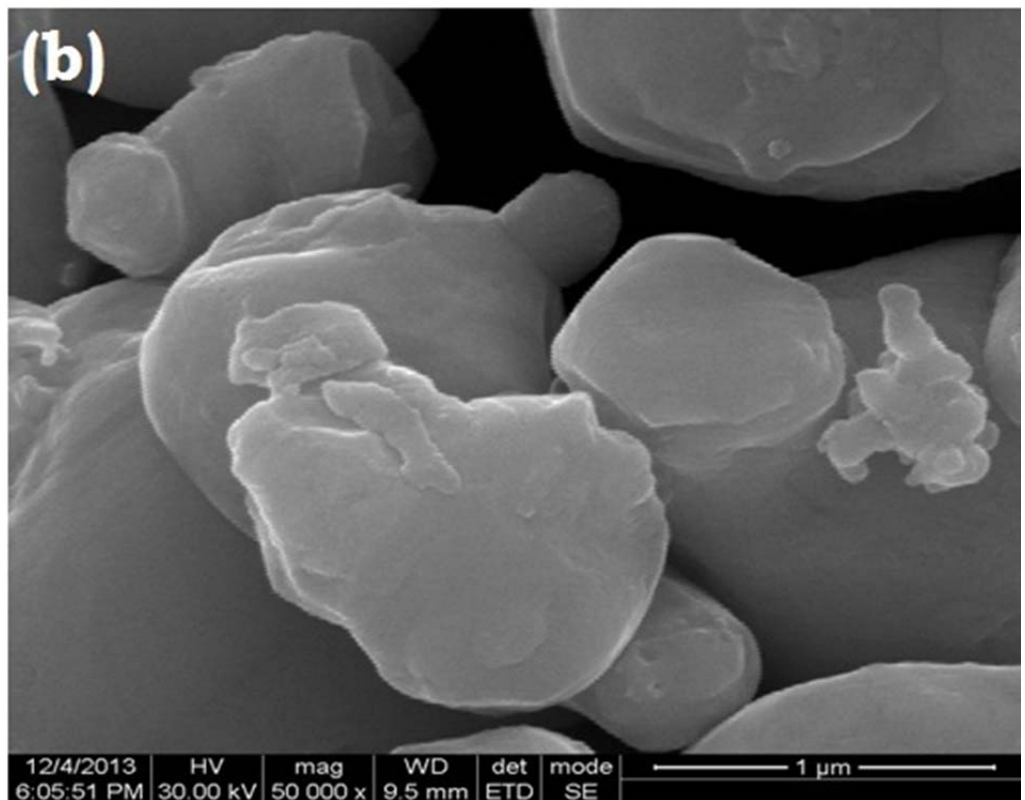
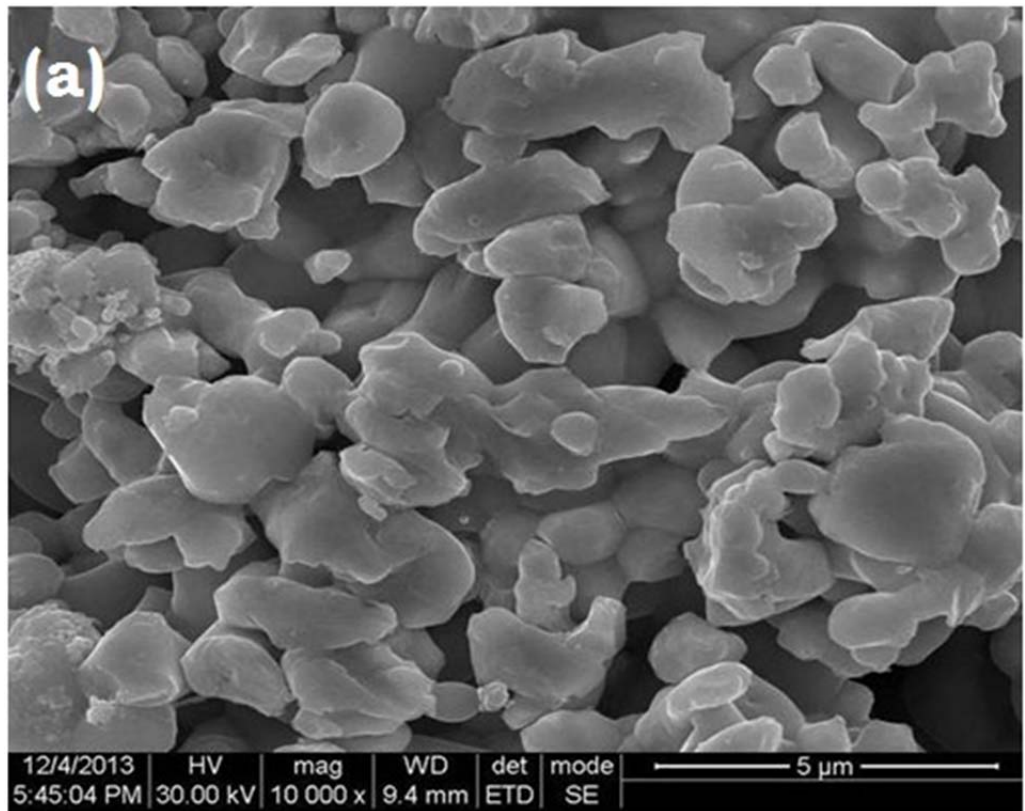


**Figure 3.4** FESEM images of prepared Ag NPs.

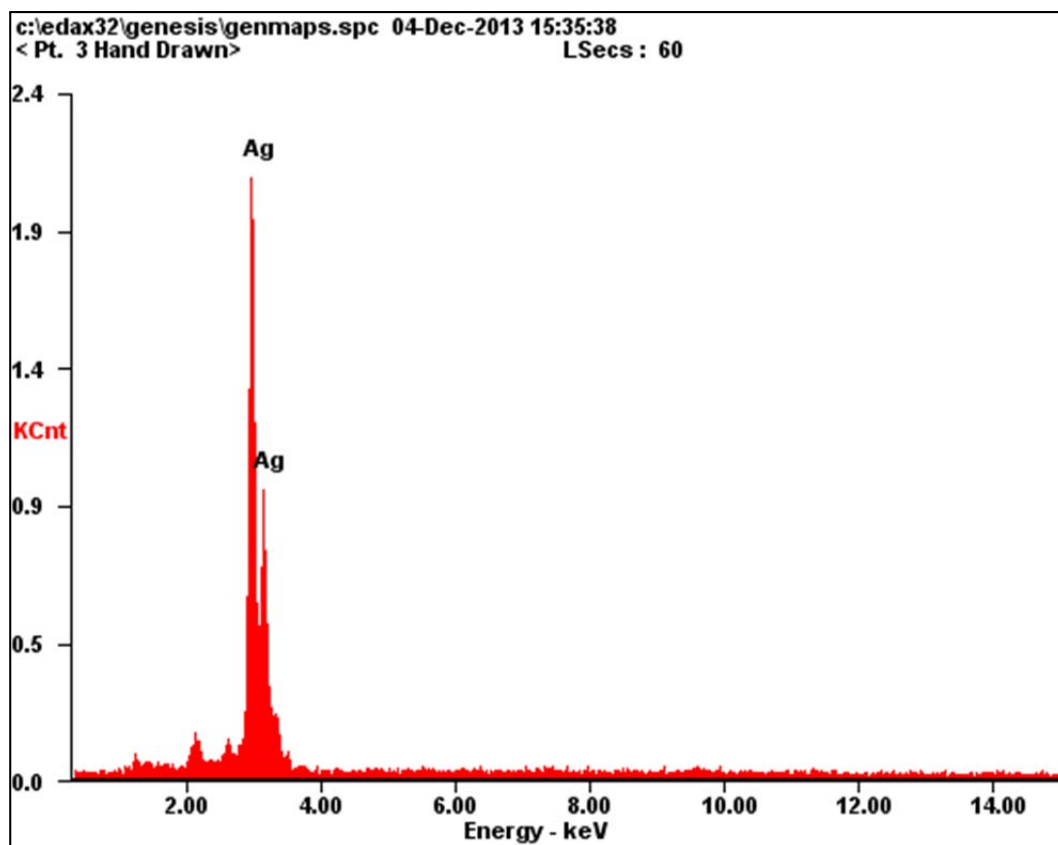


**Figure 3.5** Energy Dispersion Spectrum (EDS) of prepared AgNPs.

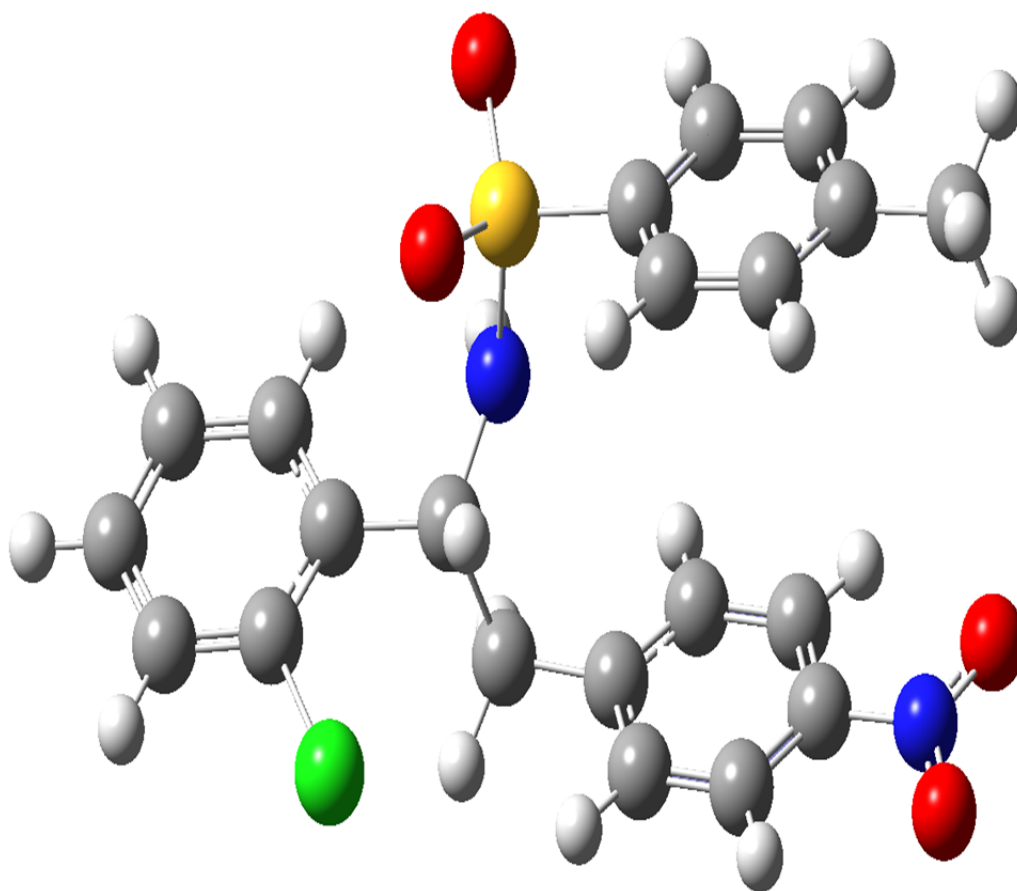


**Figure 3.6** Structure of N-(1-(2 chlorophenyl)-2-(4-nitrophenyl)ethyl)-4-methylbenzenesulfonamide (CNPSA) molecule.

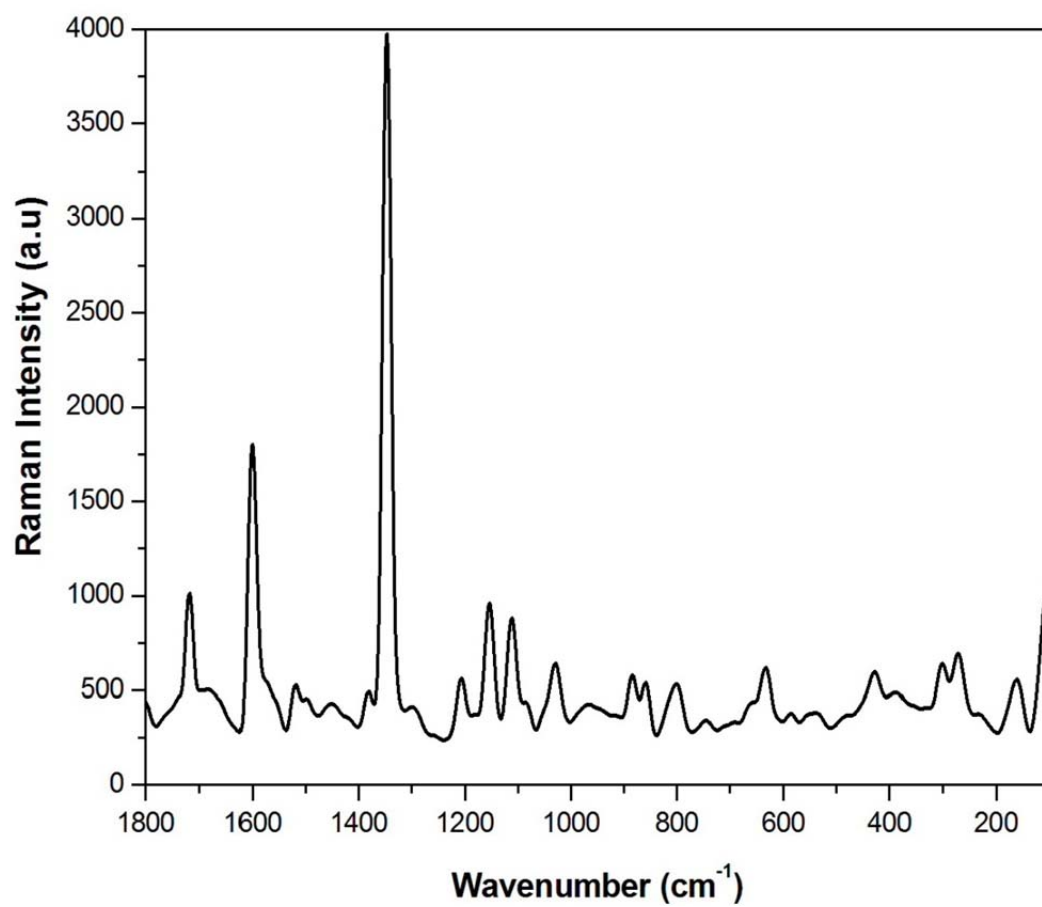


**Figure 3.7** Normal Raman spectrums (nRs) of CNPSA molecule.

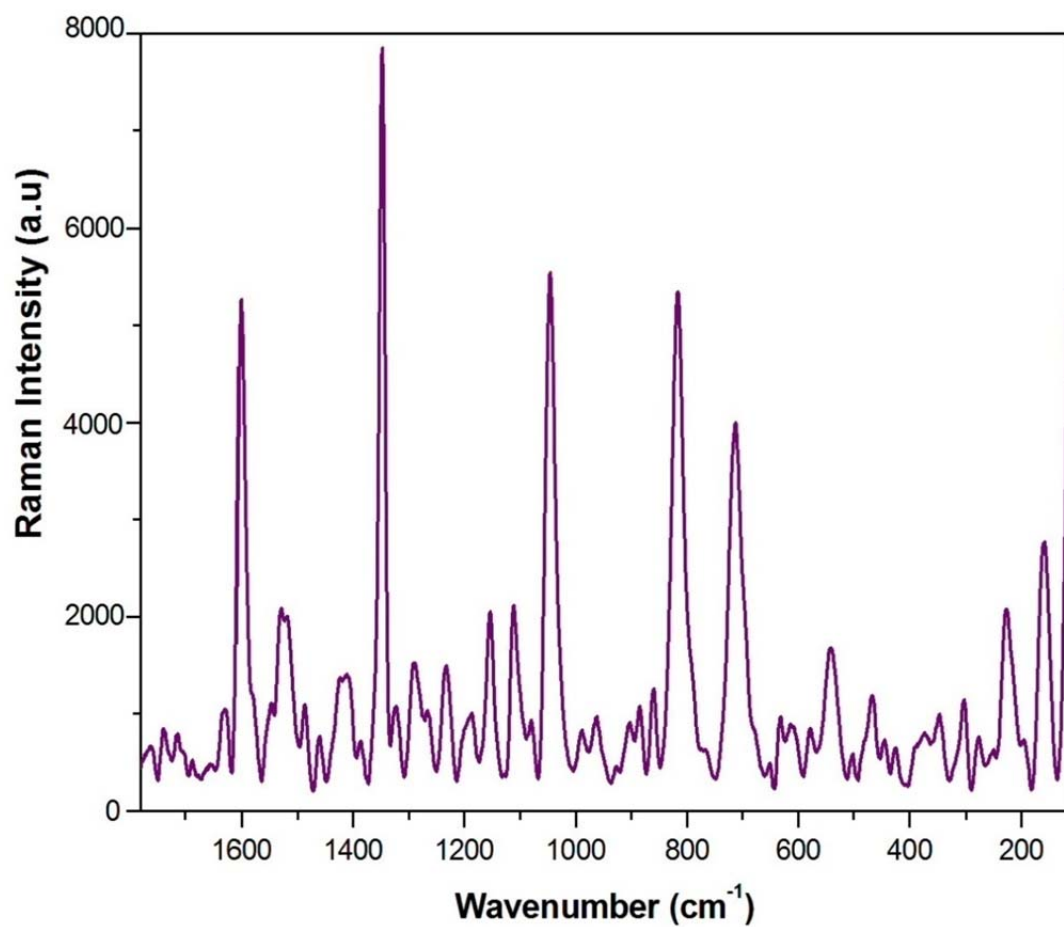


**Figure 3.8** Surface Enhanced Raman Spectrums (SERS) of CNPSA molecule on Ag NPs.

**Table 3.1.** Vibrational assignment of CNPSA and CNPSA on the Ag NPs.

Wavenumber (cm <sup>-1</sup> )		Band Assignments
nRs	SERS	
	1629	C-C str.,
1602	1602	C-C str., NH def., asy. NO <sub>2</sub> str.
	1529	C-C str., NH def, asy. NO <sub>2</sub> str.
	1417	C-C str., asy. SO <sub>2</sub> str. CH <sub>2</sub> sci.
1344	1350	C-C str., C-N str, SO str, CH <sub>2</sub> wag., sy. NO <sub>2</sub>
	1290	C-C str., C-H i.p., C-N str., CH <sub>2</sub> wag.
1207	1232	C-H i.p., sy.SO <sub>2</sub> str., CH <sub>2</sub> wag.
	1187	C-H i.p., sy. SO <sub>2</sub> str., CH <sub>2</sub> wag.
1154	1152	C-H i.p., CH <sub>2</sub> wag.
1111	1111	C-H i.p., Ring breathing
1030	1044	C-H i.p.
	990	C-H i.p.
	962	C-H o.p.
885	863	C-H o.p.
801	814	C-H o.p.
	714	C-H o.p., C-Cl str.
634		C-H o.p., C-Cl str.
	608	C-H o.p., C-Cl str.
	541	skel def., SO <sub>2</sub> def.
	466	skel .def., SO <sub>2</sub> def., Ph i.p.
427		skel. def.
	348	skel. def.
304	302	C-Cl i.p., skel def.
270	278	skel. def.
	227	Ag-O str.
161	158	CH <sub>3</sub> rock.

str. – stretching, def. – deformation, i.p. – in-plane bending, o.p. – out-of-plane bending, rock. – rocking, skel. – skeletal, as.-asymmetric, sy.-symmetric, sci.-scissoring, wag.-wagging.